







KOH-activated tire pyrolysis char as an adsorbent for chloroorganic water pollutants

Krzysztof Kuśmierk¹ , Beata Doczekalska² , Monika Bartkowiak² ,
Andrzej Świątkowski¹ , Robert Cherbański^{3*} , Tomasz Kotkowski³ 

¹ Military University of Technology, Faculty of Advanced Technologies and Chemistry, ul. Kaliskiego 2, 00-908 Warsaw, Poland

² Poznań University of Life Sciences, Department of Chemical Wood Technology, ul. Wojska Polskiego 38/42, Poznań, Poland

³ Warsaw University of Technology, Faculty of Chemical and Process Engineering, ul. Waryńskiego 1, 00-645 Warsaw, Poland

Abstract

Activated carbons (ACs) produced from end-of-life tires with different tire pyrolysis char (TPC)-to-activator (KOH) ratios of 1:2, 1:3, and 1:4 were prepared and characterized. These materials were used as adsorbents for the removal of two common chloroorganic water contaminants such as 2,4-dichlorophenol (DCP) and 2,4-dichlorophenoxyacetic acid (2,4-D). The adsorption kinetics, equilibrium adsorption, and effects of solution pH were investigated. The adsorption of both adsorbates was found to be pH-dependent and preferred in acidic environments. The adsorption kinetics was evaluated using pseudo-first-order and pseudo-second-order kinetic models and mechanism – using Weber–Morris and Boyd models. Results demonstrated that the adsorption of DCP and 2,4-D on all ACs followed the pseudo-second-order model and was controlled by film diffusion. The Langmuir isotherm described the equilibrium data better than the Freundlich isotherm model. The maximum adsorption capacity of DCP adsorbed on AC1:2, AC1:3, and AC1:4 at equilibrium was 0.582, 0.609, and 0.739 mmol/g, respectively, while the maximum adsorption capacities for 2,4-D were 0.733, 0.937, and 1.035 mmol/g, respectively. The adsorption rate and efficiency were closely correlated with the porous structure of the tested adsorbents. The results showed that the activated carbons obtained from the scrap of end-of-life tires as raw materials could be used as a low-cost and alternative adsorbent for the removal of chlorinated organic pollutants from water.

* Corresponding author, e-mail:
robert.cherbanski@pw.edu.pl

Article info:

Received: 26 July 2024

Revised: 09 November 2024

Accepted: 18 November 2024

Keywords

tire pyrolysis char, KOH activation, activated carbons, adsorption, chloroorganic water pollutants

1. INTRODUCTION

Chlorinated organic compounds are an important group of environmental pollutants. Compounds such as 2,4-dichlorophenol (DCP) and 2,4-dichlorophenoxyacetic acid (2,4-D) are model water pollutants and belong to the common environmental contaminant groups of chlorophenols (Czaplicka, 2004; Garba et al., 2019; Yadav et al., 2023) and herbicides (Blachnio et al., 2023a; Ighalo et al., 2023). Both compounds are structurally similar and differ only in the benzene ring's functional group at position 1. The 2,4-D is synthesized by the reaction of DCP with chloroacetic acid (Moszczyński and Białek, 2012). In addition, dichlorophenol can be formed as an intermediate in the degradation of 2,4-D (e.g., by oxidation (Hashimoto et al., 2010)), so both compounds are often found in the environment simultaneously. Both chlorophenols and herbicides, including DCP and 2,4-D, are widely used in industry and agriculture and enter the environment through wastewater or surface runoff from agricultural land. These contaminants end up in surface water and infiltrate through the soil into groundwater, the source of drinking water. The presence of these compounds in the aquatic environment is undesirable and often very dangerous as they are toxic to living organisms (some chlorophenols are suspected of having carcinogenic

and mutagenic properties) (Czaplicka, 2004; Yadav et al., 2023; Blachnio et al., 2023a). According to the World Health Organization (WHO, 2003a; WHO, 2003b), the median lethal dose (LD₅₀) for DCP in rats ranged from 0.6 to 4.0 mg/kg body weight. The oral LD₅₀ values for humans range from 0.4 to 2.0 g/kg of body weight, while the dermal LD₅₀ value is generally greater than 2.0 g/kg of body weight. For these reasons, removing these organochlorine compounds from water becomes an urgent and vital problem.

Several water purification methods have been developed in recent years that vary in effectiveness and cost. Undoubtedly, adsorption is currently the most popular method used to remove soluble and insoluble organic contaminants from water due to its numerous advantages, including high efficiency, simplicity of construction and application, and high versatility (Blachnio et al., 2023a; Blachnio et al., 2023b; Garba et al., 2019; Ighalo et al., 2023; Yadav et al., 2023). Naturally, adsorption efficiency is closely related to the physicochemical properties of the adsorbent used. The most commonly used adsorbents today are activated carbons, mainly due to their well-developed porous structure (high specific surface area), which generally results in their high adsorption capacity. Commercially available activated carbons



are usually expensive due to the high costs of non-renewable precursors such as wood, peat, petroleum coke, and coals (anthracite, bituminous, lignite) (Crini et al., 2019; Garba et al., 2019). Therefore, alternative raw materials (precursors) that are renewable, readily available, and cheap are sought to produce activated carbons. Various solid agricultural wastes and industrial by-products can be used as such precursors (Blachnio et al., 2023a; Blachnio et al., 2023b; Crini et al., 2019; Doczekalska et al., 2020; Doczekalska et al., 2022; Garba et al., 2019). The synthesis of activated carbons, including the choice of precursor and the activation method, is being studied by many research groups to obtain the most effective adsorbent while minimizing its production cost.

Tires are mainly composed of vulcanized natural and synthetic rubbers (45–47 wt.%), carbon (5–22 wt.%), steel (16–25 wt.%), textiles (5 wt.%), ZnO (1–2 wt.%), sulfur (1 wt.%), TiO₂ and SiO₂ (5–7.5 wt.%). Carbon is, therefore, the main element and accounts for 68–75% by weight. This chemical composition means that used tires can be a good precursor for producing activated carbons (Alexandre-Franco et al., 2011). Activated carbons from used tires are obtained in two steps, i.e., carbonization and activation. Carbonization involves annealing the waste in an inert gas atmosphere at about 800 °C. The pyrolytic carbon is then subjected to activation, the purpose of which is to develop a porous structure.

Activation can be carried out by physical or chemical methods. For activated carbons from used tires, the most common method is physical activation using steam at 800–900 °C. Less frequently, CO₂ is used in activation processes. It was found that steam activation results in activated carbons with a very well-developed specific surface area of about 1000 m²/g. In contrast, activated carbons obtained by activation with carbon dioxide had S_{BET} in the range of 270–980 m²/g (Mui et al., 2004; Muttill et al., 2023). Chemical activation processes, on the other hand, use chemicals such as NaOH, KOH, H₃PO₄, and ZnCl₂, and the process is carried out in the absence of air at temperatures ranging from 500 to 900 °C. The solids showed an area between 42 and 528 m²/g with characteristic

isotherms of micro-mesoporous solids and a chemical surface with acid and basic groups (Ramirez-Arias et al., 2020). However, the chemical activation process is more advantageous than the physical activation process, as the former produces a higher yield and pore volumes. The utilization of chemicals reduces the formation of tar and by-products during the pyrolysis process (Muttill et al., 2023).

Activated carbons from end-of-life tires, produced via physical or chemical activation, have found a wide range of applications, e.g., in hydrogen storage and energy storage devices (Muttill et al., 2023; Zerin et al., 2023; Zerin et al., 2024) or as adsorbents for the removal of environmental pollutants from both the gaseous phase (atmospheric purification) and the liquid phase (water and wastewater treatment) (Ali et al., 2022; Jones et al., 2021; Kuśmierek et al., 2021a; Kuśmierek et al., 2021b; Mui et al., 2004; Muttill et al., 2023).

This work aimed to study the adsorption of 2,4-dichlorophenol (DCP) and 2,4-dichlorophenoxyacetic acid (2,4-D) from water on activated carbons produced from end-of-life tires. Adsorption kinetics, equilibrium adsorption, and the effect of solution pH were investigated.

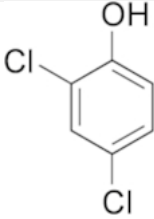
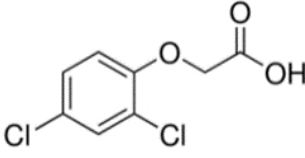
2. EXPERIMENTAL

2.1. Reagents and materials

The 2,4-dichlorophenol, > 99%, (DCP) was from Sigma-Aldrich (St. Louis, MO, USA), and 2,4-dichlorophenoxyacetic acid, > 99%, (2,4-D) was from Acros Organics (Geel, Belgium). The main physicochemical properties of these compounds are listed in Table 1. Other high-purity reagents were obtained from Chempur (Piekary Śląskie, Poland).

Tire pyrolysis char (TPC) was fabricated in a pilot plant from shredded end-of-life tires of different types and brands (Kuśmierek et al., 2020a). The feedstock was fed to a batch tank reactor and pyrolyzed at 500 °C in a nitrogen atmosphere. The TPC yielded 39 wt.%.

Table 1. Physicochemical properties of 2,4-dichlorophenol (DCP) and 2,4-dichlorophenoxyacetic acid (2,4-D).

Parameter	DCP	2,4-D
CAS No.	120-83-2	94-75-7
Chemical structure		
Molecular size [Å]	4.82 × 6.47	4.88 × 9.49
Molecular weight [g/mol]	163.00	221.04
Water solubility at 20 °C [g/L]	4.50	0.682
pKa	7.80	2.98

2.2. Preparation and characterization of activated carbons

Chemical activation was carried out in an electric furnace (Czylok, Jastrzębie Zdrój, Poland) using KOH. The space in which the activation process occurred was a ceramic tube resistant to acid-base reactants and high temperatures and pressures. In the first stage, TPC was ground in a ceramic mortar with potassium hydroxide at the following TPC/KOH weight ratios: 1:2, 1:3, and 1:4. The mixture was then placed in nickel containers and placed in an oven at 850 °C. Activation was carried out in an atmosphere of argon flowing at a rate of 20 dm³/h for 15 minutes. After the process was completed, the carbon material was quantitatively transferred to a cellulose thimble and extracted in a Soxhlet apparatus with 2% hydrochloric acid for 8 h, followed by 8 h with distilled water. Finally, the activated carbon was dried at 105 °C to a constant weight (about 12 h). The resulting activated carbons were designated in the paper by the following abbreviations: AC1:2, AC1:3, and AC1:4. Prior to adsorption experiments, all of the ACs were dried in an oven at 120 °C to a constant weight and then stored in a desiccator until they were used.

The porous structure of obtained activated carbons was characterized using low-temperature nitrogen adsorption analysis. The N₂ adsorption–desorption isotherms were performed on ASAP 2020 analyzer (Micromeritics, Norcross, GA, USA) at a temperature of 77 K. Samples before measurement were degassed at 300 °C for 10 hours at pressure 1 · 10⁻⁶ Pa. The specific surface area, volume of micro- and mesopores, and average pore diameter were calculated. The specific surface areas (*S*_{BET}, m²/g) were calculated according to the Brunauer–Emmett–Teller method at relative pressure $p/p_0 \approx 0.05 - 0.2$. The total pore volume (*V*_t, cm³/g) was determined from the adsorption isotherm at relative pressure $p/p_0 \approx 0.95$. The micropore volume (*V*_{mi}, cm³/g) and mesopore volume (*V*_{me}, cm³/g) were also determined using the Barrett–Joyner–Halenda and *t*-plot methods. The average pore diameter *d*_A (nm) was calculated from the following formula: $4V_t/S_{BET}$.

Contents of surface functional oxygen groups for three obtained activated carbons were determined according to Boehm's method (Boehm, 2008). Four samples (250 mg) from each of them were supplemented with 25 mL of 0.1 mol/L NaOH, 0.1 mol/L NaHCO₃, or 0.05 mol/L Na₂CO₃ (to assay acidic groups i.e., carboxyl groups, lactones, phenol, and lactol groups) or 0.1 mol/L HCl (to assay basic groups i.e., chromene, diketone, quinone, pyrone, and nitrogen-containing groups).

After shaking at 120 rpm for 24 h at room temperature, the filtered mixtures (10 mL of each filtrate) were pipetted, and the excess of bases or acid was titrated using 0.1 mol/L HCl or NaOH, respectively. The point of zero charge (pH_{PZC}) of the activated carbons was measured using the pH drift method.

The thermogravimetric analysis (recording of TG curves) carried out on an STA 449 F5 Jupiter-QMS of the NETZSCH (Burlington, MA, USA) apparatus was employed to analyze the population of surface functional groups. The following

conditions were used: final temperature 900 °C, rate of temperature increase: 5 °C/min, atmosphere: helium flowing at about 1.5 dm³/h.

2.3. Batch adsorption experiments

Adsorption studies of DCP and 2,4-D on activated carbons were carried out in Erlenmeyer flasks, to which 20 mL of adsorbate solution of the appropriate concentration and 0.01 g of weighed AC were added. The mixtures thus prepared were shaken on a laboratory shaker at a constant speed of 150 rpm at 23 °C. After 8 hours (equilibrium and pH studies) or after an appropriate time (kinetic studies), the solutions were filtered through filter paper, and the amount of adsorbate remaining in the solution was measured. All adsorption experiments were performed twice, and the average value was used to calculate the results. The effects of solution pH, adsorption kinetics, and adsorption under equilibrium conditions (adsorption isotherms) were investigated. In the first two cases, experiments were carried out for DCP and 2,4-D solutions with initial concentrations of 0.5 mmol/L. Adsorption isotherms were obtained for adsorbate solutions with initial concentrations of 0.3 to 1.0 mmol/L. These studies were carried out in solutions of the adsorbates at their original pH (~ 5.90 for DCP and ~ 3.40 for 2,4-D). For studies on the effect of pH on adsorption, the adsorbate solutions were adjusted to the appropriate pH by adding small amounts of 0.01 mol/L NaOH or HCl. The amount of adsorbate adsorbed after time *t* (*q*_{*t*}) and under equilibrium conditions (*q*_{*e*}) was calculated from the following equations:

$$q_t = \frac{(C_0 - C_t)V}{m} \quad (1)$$

$$q_e = \frac{(C_0 - C_e)V}{m} \quad (2)$$

The adsorption efficiency (%) was calculated as follows:

$$\text{Adsorption (\%)} = \frac{(C_0 - C_e)}{C_0} \times 100 \quad (3)$$

The concentrations of DCP and 2,4-D in solution were determined spectrophotometrically (Varian Carry 3E spectrophotometer, Palo Alto, CA, USA) at 283 nm. The calibration curves for the determination of both adsorbates were linear over the concentration range tested (0.05–0.8 mmol/L) and were described by the following equations: $y = 1.753x + 0.037$ ($R^2 = 0.997$) for DCP and $y = 1.590x + 0.064$ ($R^2 = 0.995$) for 2,4-D.

3. RESULTS AND DISCUSSION

3.1. Characteristics of the activated carbons

The obtained adsorption–desorption isotherms and pore size distribution are presented in Fig. 1. The calculated porous structure parameters of activated carbons (specific surface area and micro- and mesopore volume) are listed in Table 2.

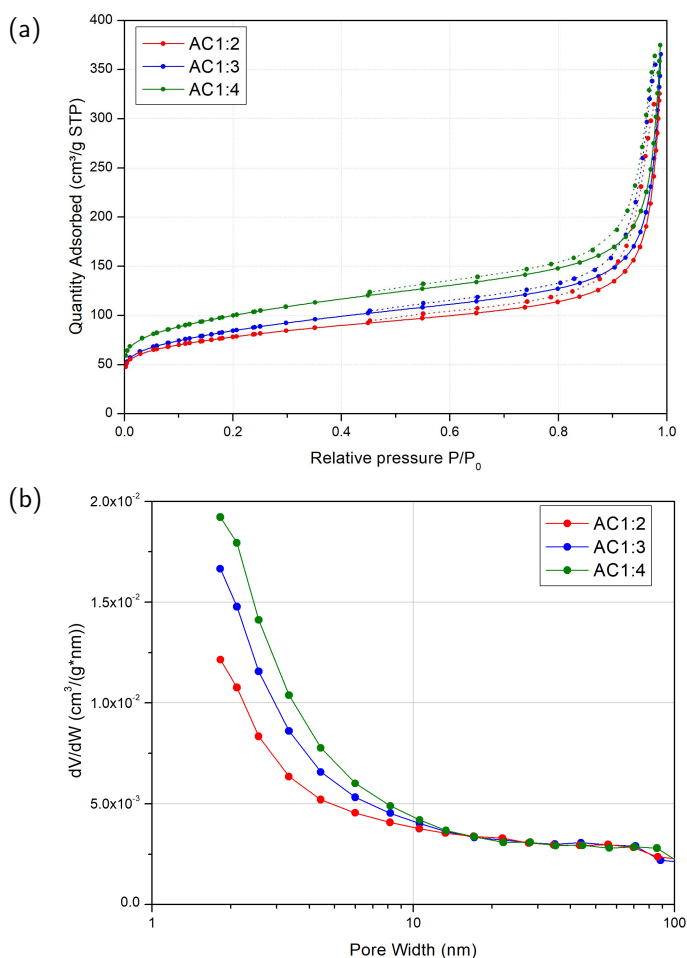


Figure 1. Nitrogen physisorption isotherms for ACs produced from end-of-life tires at 77 K (a) and pore size distribution (b).

Table 2. Textural characteristics of the activated carbons produced from end-of-life tires.

Activated carbon	S_{BET} [m ² /g]	C_{BET}	V_{mi} [cm ³ /g]	V_{t} [cm ³ /g]	V_{me} [cm ³ /g]	$d_A = 4V_{\text{t}}/S_{\text{BET}}$ [nm]
AC1:2	277	310	0.126	0.414	0.288	5.98
AC1:3	298	315	0.137	0.444	0.307	5.96
AC1:4	352	195	0.163	0.477	0.314	5.42

As can be seen, an increase in the TPC to activating agent (KOH) ratio results in an increase in the specific surface area as well as the micropore and mesopore volumes. In contrast, the average pore diameter (d_A) decreased. Similarly, the increase of the TPC:KOH proportion significantly increases the content of surface oxygen functional groups (acidic as well basic) – Table 3. Such observations can be seen in other papers (Jedynak et al., 2024; Nandi et al., 2023; Zhang et al., 2017).

Table 3. Surface chemistry characteristics of the ACs produced from end-of-life tires.

Activated carbon	Ash content [wt.%]	Total acidic groups [mmol/g]	Total basic groups [mmol/g]	pHpzc
AC1:2	8.05	0.79	0.70	6.30
AC1:3	8.65	0.86	0.77	6.50
AC1:4	9.06	0.94	0.87	6.60

Results of the thermogravimetric analysis performed for investigated activated carbons are presented as TG curves in Figure 2.

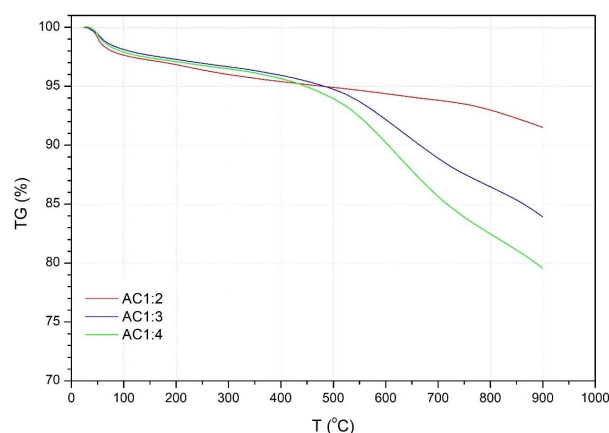


Figure 2. TG curves of activated carbons obtained from end-of-life tires.

The observed mass loss values, at a temperature of 900 °C, taking into account and subtracting from their values mass losses due to water evaporation (release of physically sorbed water) up to temperature of approximately 250 °C, were as follows: 5, 13, and 16.5 %wt. for AC1:2, AC1:3 and AC1:4, respectively. The mass losses mainly correspond to the thermal decomposition of surface oxygen functional groups. Some papers in the literature (Szymański et al., 2002) describe the decomposition temperature ranges of various surface groups. At lower temperatures (Fig. 2), 300–400 °C – carboxylic, 400–650 °C – lactone, and 550–700 °C – phenolic groups are destroyed.

3.2. Adsorption study

3.2.1. Adsorption kinetics

The adsorption kinetics of DCP and 2,4-D on activated carbons is shown in Fig. 3. Initially, both adsorbates were adsorbed very rapidly (about 70–80% was adsorbed in the first 30 min). Then, the adsorption rate decreased, reaching equilibrium after about 120 min.

Several theoretical models were used to describe the experimental data obtained, including the pseudo-first-order (PFO, Eq. (4)) and pseudo-second-order (PSO, Eq. (5)), the Weber-Morris (Eq. (6)) and the Boyd (Eqs. (7) and (8)) (Nasser et al., 2024; Tan and Hameed, 2017):

$$\log(q_e - q_t) = \log q_e - \frac{k_1}{2.303} t \quad (4)$$

$$\frac{t}{q_t} = \frac{1}{k_2 q_e^2} + \frac{1}{q_e} t \quad (5)$$

$$q_t = k_f t^{0.5} + C_i \quad (6)$$

$$B_T = \pi \left(1 - \sqrt{1 - \frac{\pi q_t}{3 q_e}} \right)^2 \quad \text{when} \quad \frac{q_t}{q_e} < 0.85 \quad (7)$$

$$B_T = -0.4977 - \ln \left(1 - \frac{q_t}{q_e} \right) \quad \text{when} \quad \frac{q_t}{q_e} > 0.85 \quad (8)$$

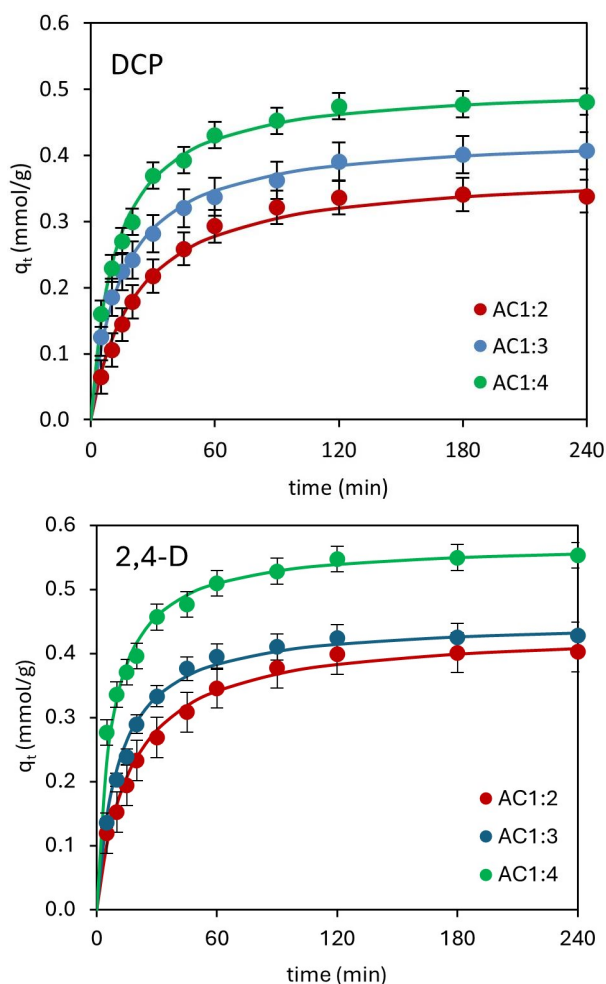


Figure 3. Adsorption kinetics of DCP and 2,4-D on ACs produced from end-of-life tires (lines mean the fitting of the pseudo-second-order kinetic model). Experimental conditions: adsorbate initial concentration = 0.5 mmol/L, AC dosage = 0.5 g/L, pH = original (~ 5.90 for DCP and ~ 3.40 for 2,4-D), temperature = 23 °C.

The values of the rate constants of the PFO and PSO equations were determined from the slope and intercept obtained for the plot of $\log(q_e - q_t) = f(t)$ and $t/q_t = f(t)$, respectively. The calculated values of k_1 and k_2 , as well as the adsorption capacities $q_{e(\text{cal})}$ (calculated) and $q_{e(\text{exp})}$ (experimental), are given in Table 4. The choice of the model that better described the experimental data was based on the analysis of the values of the determination coefficients (R^2) and chi-square (χ^2):

$$R^2 = \left(\frac{\sum_{i=1}^n (q_{e(\text{cal}),i} - \bar{q}_{\text{cal}})(q_{e(\text{exp}),i} - \bar{q}_{e(\text{exp})})}{\sqrt{\sum_{i=1}^n (q_{e(\text{cal}),i} - \bar{q}_{\text{cal}})^2} \sqrt{\sum_{i=1}^n (q_{e(\text{exp}),i} - \bar{q}_{e(\text{exp})})^2}} \right)^2 \quad (9)$$

$$\chi^2 = \sum_{i=1}^n \frac{(q_{e(\text{exp})} - \bar{q}_{e(\text{cal})})^2}{q_{e(\text{cal})}} \quad (10)$$

Higher R^2 values (closer to 1) and lower χ^2 values indicate a better fit of the model used. As can be seen in Table 4, higher R^2 values (≥ 0.997) and lower χ^2 values (≤ 0.0116) were obtained for the PSO model than for PFO. Thus, it can be

Table 4. Kinetic modeling data for the adsorption of DCP and 2,4-D on ACs produced from end-of-life tires.

Kinetic model	Adsorbent/Adsorbate		
	AC1:2	AC1:3	AC1:4
DCP			
$q_{e(\text{exp})}$ [mmol/g]	0.338	0.406	0.481
Pseudo-first-order			
k_1 [1/min]	0.0386	0.0226	0.0338
$q_{e1(\text{cal})}$ [mmol/g]	0.369	0.284	0.407
R^2	0.974	0.951	0.954
χ^2	0.191	1.503	0.508
Pseudo-second-order			
k_2 [g/mmol/min]	0.122	0.157	0.165
$q_{e2(\text{cal})}$ [mmol/g]	0.378	0.432	0.508
R^2	0.997	0.999	0.999
χ^2	0.0057	0.0043	0.0033
2,4-D			
$q_{e(\text{exp})}$ [mmol/g]	0.402	0.428	0.553
Pseudo-first-order			
k_1 [1/min]	0.0327	0.0352	0.0334
$q_{e1(\text{cal})}$ [mmol/g]	0.358	0.329	0.360
R^2	0.973	0.958	0.949
χ^2	0.184	0.685	2.973
Pseudo-second-order			
k_2 [g/mmol/min]	0.138	0.208	0.235
$q_{e2(\text{cal})}$ [mmol/g]	0.436	0.451	0.572
R^2	0.998	0.999	0.997
χ^2	0.0070	0.0051	0.0116

concluded that the adsorption kinetics of both DCP and 2,4-D on all three activated carbons follows the pseudo-second-order model. By analyzing the obtained values of the rate constants k_2 , it can be seen that both adsorbates adsorbed fastest on AC1:4 and slowest on AC1:2 ($AC1:2 < AC1:3 < AC1:4$). The observed order appears to be correlated with the porous structure of the ACs tested as shown in Table 2.

The classification recommended by IUPAC (Thommes et al., 2015) distinguishes between macropores (width higher than 50 nm), mesopores (width between 2 nm and 50 nm), and micropores (width not greater than about 2 nm). The function of the pores in the adsorption process varies according to their size. The micropores are responsible for the adsorption capacity of the adsorbent since it is in the micropores that the actual adsorption, understood as binding the adsorbate molecules to the surface of the adsorbent (surface reaction), takes place. A well-developed microporous structure (high micropore volume) is generally associated with an excellent adsorption capacity of the adsorbent. Adsorbate molecules can also bind to the surface of the adsorbent in mesopores and macropores. However, these pores primarily have a transport function. Mesopores and macropores are 'highways' through which adsorbate molecules enter the micropores. In general, the kinetic properties of the adsorbent – its ability to take up adsorbate molecules from solution more rapidly – are improved by the larger volume of mesopores and their more significant contribution to the total pore volume. The adsorption rate of DCP and 2,4-D observed in the present study ($AC1:2 < AC1:3 < AC1:4$) is related to the mesopore volume of the activated carbons. The adsorption rate increases with the increase in the mesopore volume of the ACs.

The PFO and PSO models (sometimes referred to as "reaction models") reveal the rate of adsorbate uptake by adsorbents, but they do not show the actual cause of adsorption. This is because several stages can be identified in the adsorption process from the liquid phase: (1) diffusion of the adsorbate molecules through the liquid film surrounding the adsorbent particles (film diffusion), (2) intraparticle diffusion (pore diffusion) when the adsorbate molecules penetrate the intraparticle spaces and pores of the adsorbent, (3) binding of the adsorbate molecules to the active sites of the adsorbent. The last, third stage, is high-speed and does not affect the adsorption rate, as the slowest stage determines the rate of the whole process. It is usually the first stage (film diffusion), the second stage (intraparticle diffusion), or a combination of both that controls the rate of the overall adsorption process (Nasser et al., 2024; Tan and Hameed, 2017).

Therefore, to better understand the adsorption kinetics of DCP and 2,4-D on the ACs, the Weber–Morris and Boyd kinetic models were applied. These two diffusion models are helpful to understand the mechanism of adsorption and to identify the rate-limiting step in the overall adsorption process.

The intraparticle diffusion kinetics for DCP and 2,4-D on the tested ACs are shown in Fig. 4 and Fig. 5, respectively.

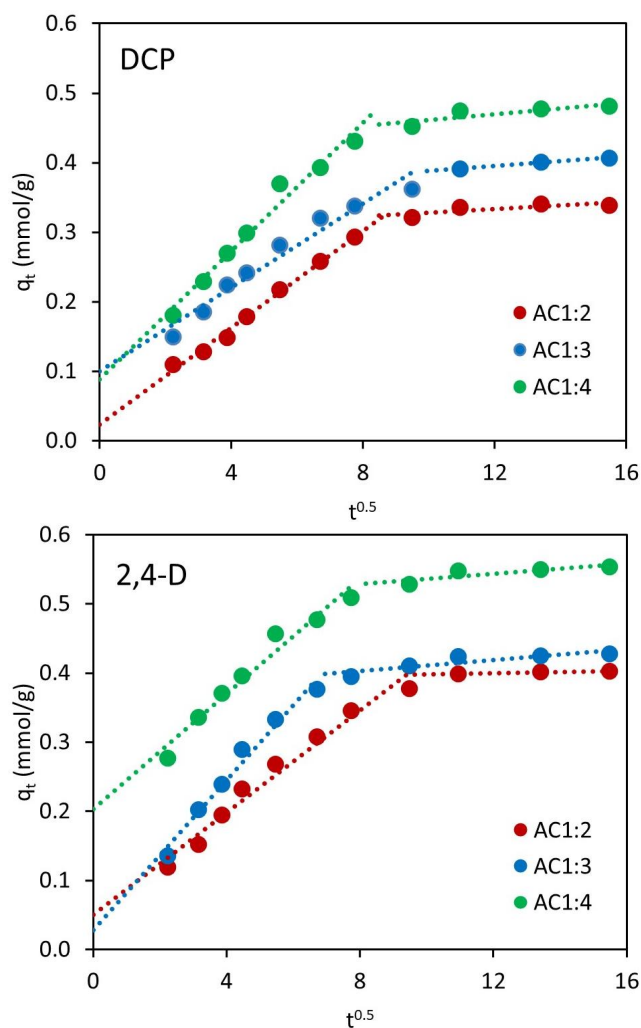


Figure 4. Intraparticle diffusion model plots for adsorption of DCP and 2,4-D on the ACs.

The Weber–Morris intraparticle diffusion model assumes that when the function $q_t = f(t^{0.5})$ is linear and passes through the origin, adsorption proceeds only by intraparticle diffusion. On the other hand, when the function is linear but does not pass through the origin, intraparticle diffusion determines the adsorption, but it is not the only step determining the process rate (Nasser et al., 2024; Tan and Hameed, 2017). Fig. 4 shows that none of the lines cross the origin and that the function is non-linear over the whole range. It is therefore concluded that intraparticle diffusion is not the only stage determining the adsorption process on the ACs and that the adsorption of both the DCP and 2,4-D is a multi-stage process. These findings also confirm the results obtained for the Boyd model (Fig. 5).

The kinetic model proposed by Boyd assumes that the thin liquid layer on the adsorbent surface has the strongest influence on the diffusion of the solute. Thus, if the graph of $B_T = f(t)$ is non-linear (or linear) and does not pass through the origin, then film diffusion will be the main determining factor of adsorption. In contrast, if the graph of $B_T = f(t)$ is

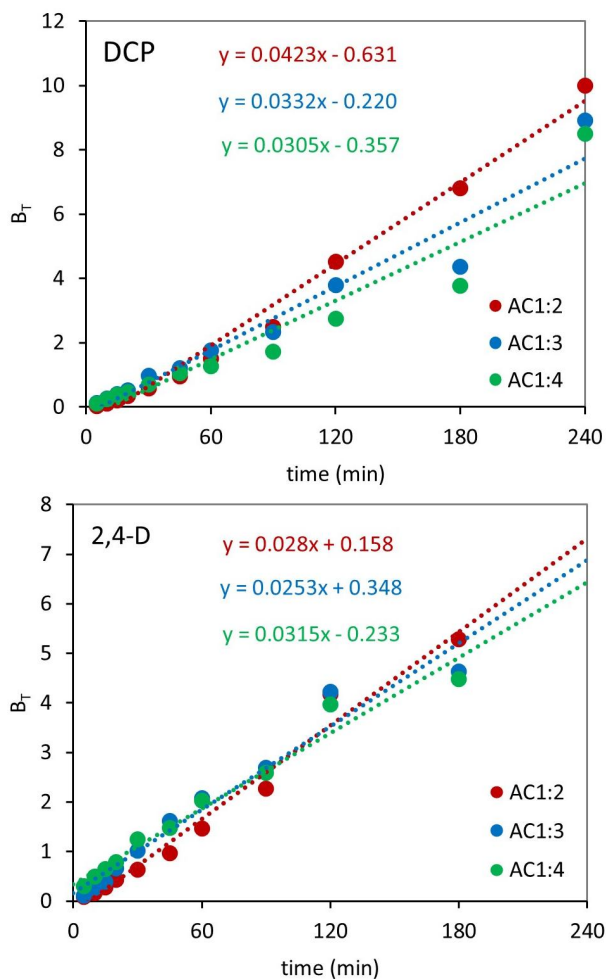


Figure 5. The Boyd kinetic model plots for adsorption of DCP and 2,4-D on the ACs.

a straight line and passes through the origin (intercept = 0), then adsorption is controlled by the intraparticle diffusion mechanism (Nasser et al., 2024; Tan and Hameed, 2017).

From the Boyd plot (Fig. 5), it can be seen that none of the curves pass through the origin, suggesting that the adsorption of both the DCP and 2,4-D on the scrap tire-derived activated carbons is a complex process affected by both intraparticle diffusion and film diffusion. However, film diffusion is the more critical step in determining the rate of the whole adsorption process.

3.2.2. Adsorption isotherms

The adsorption isotherms of DCP and 2,4-D on activated carbons from end-of-life tires are shown in Fig. 6.

Two most commonly used isotherm models, Freundlich and Langmuir, were used to describe the experimental data (Hamdaoui and Naffrechoux, 2007). The Freundlich model, whose linear form is given by Equation (11), assumes multilayer adsorption on a heterogeneous surface. In contrast, the Langmuir model, whose linear form is expressed by Equation (12),

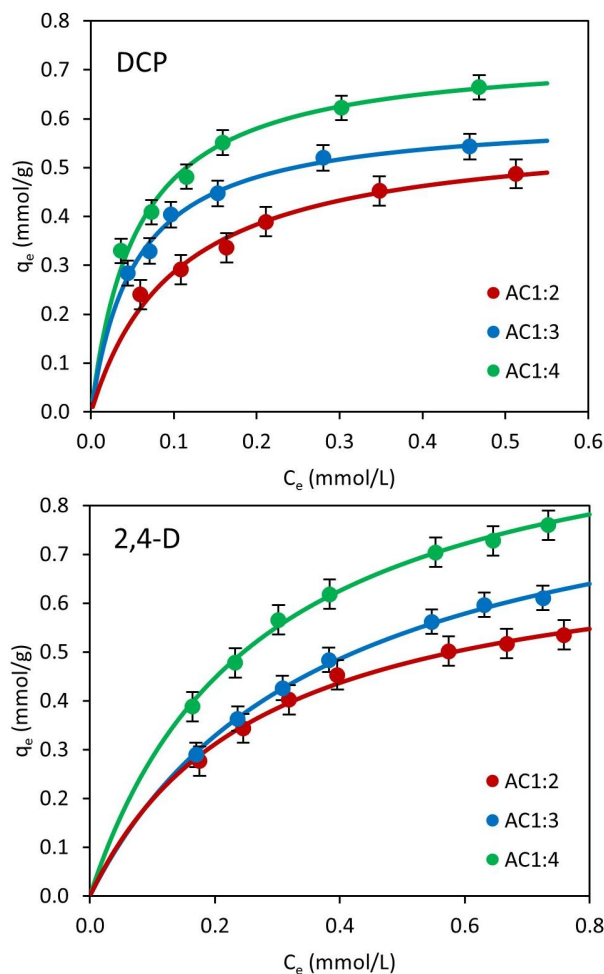


Figure 6. Adsorption isotherms of DCP and 2,4-D on ACs produced from end-of-life tires (lines represent the Langmuir isotherm fitting). Experimental conditions: DCP and 2,4-D initial concentrations from 0.3 to 1.0 mmol/L, AC dosage = 0.5 g/L, pH = original (~ 5.90 for DCP and ~ 3.40 for 2,4-D), temperature = 23°C .

assumes monolayer adsorption on a homogeneous surface.

$$\ln q_e = \ln K_F + \frac{1}{n} \ln C_e \quad (11)$$

$$\frac{C_e}{q_e} = \frac{1}{q_m} C_e + \frac{1}{q_m K_L} \quad (12)$$

These isotherm parameters were calculated from the slope and intercept obtained for the linear relationship $\ln q_e$ vs. $\ln C_e$ for the Freundlich model and C_e/q_e vs. C_e for the Langmuir model. The suitability of a given model to describe the experimental data was based on the analysis of R^2 and χ^2 values. The results are listed in Table 5.

As can be seen in Table 5, higher R^2 values and, at the same time, lower χ^2 values were obtained for the Langmuir model, indicating that this model better describes the experimental data. The better fit of the Langmuir model also suggests monolayer adsorption of both adsorbates on homogeneous surfaces of the activated carbons.

Table 5. The Freundlich and Langmuir isotherm constants for the adsorption of DCP and 2,4-D on ACs.

Isotherm model	Adsorbent/Adsorbate		
	AC1:2	AC1:3	AC1:4
DCP			
Freundlich			
K_F [(mmol/g)(L/mmol) ^{1/n}]	0.604	0.726	0.866
1/n	0.343	0.285	0.282
R^2	0.988	0.944	0.975
χ^2	0.990	1.025	0.809
Langmuir			
q_m [mmol/g]	0.582	0.609	0.739
K_L [L/mmol]	9.727	18.78	18.19
R^2	0.996	0.999	0.999
χ^2	0.059	0.022	0.033
2,4-D			
Freundlich			
K_F [(mmol/g)(L/mmol) ^{1/n}]	0.633	0.788	0.927
1/n	0.438	0.545	0.457
R^2	0.959	0.989	0.973
χ^2	1.558	0.778	0.857
Langmuir			
q_m [mmol/g]	0.733	0.937	1.035
K_L [L/mmol]	3.688	2.697	3.774
R^2	0.996	0.997	0.998
χ^2	0.068	0.031	0.044

The Langmuir constant K_L can be used to determine the separation factor (R_L) (Hamdaoui and Naffrechoux, 2007) as well as the Gibbs free energy of change (ΔG°) (Zhou and Zhou, 2014) by the following formulas:

$$R_L = \frac{1}{1 + K_L C_0} \quad (13)$$

$$\Delta G^\circ = -RT \ln(55.5 K_L) \quad (14)$$

The separation factor characterizes the nature of the adsorption. So, depending on the value of the R_L , the adsorption may be irreversible ($R_L = 0$), linear ($R_L > 1$), unfavorable ($R_L > 1$), or favorable ($0 < R_L < 1$) (Hamdaoui and Naffrechoux, 2007).

The R_L calculated for DCP and 2,4-D on all three activated carbons were in the range of 0.052–0.225 and 0.209–0.553, respectively. Separation factor values less than one and greater than zero indicate favorable adsorption.

The Gibbs free energy of change measures the spontaneity and feasibility of the adsorption process. A negative value of ΔG° confirms that the process is spontaneous. The calculated ΔG° values for AC1:2, AC1:3, and AC1:4 were –32.5, –34.1, and –34.0 kJ/mol for DCP and –30.1, –29.3 and –30.2 kJ/mol for 2,4-D, respectively. These results confirm the spontaneous nature of the adsorption.

In the case of each activated carbon, it was observed that 2,4-D was better adsorbed than DCP. The herbicide molecule is larger and "heavier" (has a higher molecular weight) and, perhaps most importantly, is less soluble in water than chlorophenol. The lower solubility means that 2,4-D is more hydrophobic than DCP. The more hydrophobic compound has a higher affinity for the hydrophobic surface of the activated carbon, which explains the better adsorption of the herbicide. Such a phenomenon is consistent with other literature reports (Białek et al., 2017; Kuśmierk et al., 2016). 2,4-D was adsorbed better than DCP on, among others, carbon blacks (Kuśmierk et al., 2016), carbonaceous materials obtained by combustion synthesis (Kuśmierk et al., 2016), and commercially available activated carbons (Białek et al., 2017).

Both DCP and 2,4-D adsorbed best on AC1:4 and weakest on AC1:2. This order (AC1:2 < AC1:3 < AC1:4) is closely correlated with the porous structure of the activated carbons (with their micropore volume and specific surface area). A higher micropore volume and a higher BET surface area mean more active sites to which adsorbate molecules can attach, resulting in enhanced adsorption efficiency. AC1:4 exhibited the highest BET surface area ($S_{BET} = 352 \text{ m}^2/\text{g}$), while AC1:2 demonstrated the lowest ($277 \text{ m}^2/\text{g}$).

Adsorption on activated carbon depends not only on its porous structure but also on its surface chemistry (the type and number of functional groups on the surface). The surface chemistry of these activated carbons from end-of-life tires was characterized using the Boehm method and TG analysis (Section (3.1)). The results obtained showed no significant differences between these ACs. The surface chemistry of these ACs was comparable, and therefore, its effect on the adsorption of the two adsorbates was practically the same for each of the three ACs tested. This suggests that the observed differences in the adsorption capacities of the activated carbons are due to differences in their porous structure (which plays a key role) rather than surface chemistry.

The adsorption mechanism of phenolic compounds (DCP) and phenoxyacetic herbicides (2,4-D) on activated carbons was the subject of many studies, which were summarized and discussed in many review papers (Blachnio et al., 2023a; Blachnio et al., 2023b; Dąbrowski et al., 2005; Garba et al., 2019; Ighalo et al., 2023). The adsorption of chlorophenols on activated carbons results from π - π dispersion interactions, electron donor-acceptor complex formation, and hydrogen bonding interactions (Dąbrowski et al., 2005; Garba et al., 2019). The most typical and essential forces driving the adsorption of

2,4-D on activated carbon include electrostatic (attractive and repulsive) interactions, $\pi - \pi$ and hydrophobic interactions, and hydrogen bond formation (Blachnio et al., 2023b; Ighalo et al., 2023). As expected, the adsorption of DCP and 2,4-D on activated carbons prepared from end-of-life tires also followed such mechanisms.

A comparison with other adsorbents is necessary to assess the suitability of ACs produced from end-of-life tires for removing both adsorbates. This comparison is shown in Table 6, which lists the adsorption capacities of various other carbonaceous adsorbents. As can be seen, the adsorption capacities of the ACs described in this paper are satisfactory.

3.2.3. Effect of solution pH

Adsorption is affected not only by the properties of the adsorbate and adsorbent but also by the properties of the solution, especially its pH. The solution's pH affects the adsorbate's

dissociation and the adsorbent's surface charge. The parameter that characterizes the surface charge on the adsorbent is the pH point of zero charge (pHpzc), defined as the pH value and the conditions of the solution at which the surface charge density of the adsorbent is equal to zero. Thus, in a solution with $\text{pH} = \text{pHpzc}$, the surface of the adsorbent is electrically neutral. When $\text{pH} < \text{pHpzc}$, the surface of the adsorbent is positively charged, and finally, when $\text{pH} > \text{pHpzc}$, a negative charge accumulates on the adsorbent surface. The pHpzc values for all three activated carbons determined according to the procedure described elsewhere (Kuśmierek et al., 2016) were 6.30 for AC1:2, 6.50 for AC1:3, and 6.60 for AC1:4.

The effect of solution pH on adsorbate dissociation depends on its pKa. The pKa values of DCP and 2,4-D are 7.80 and 2.98, respectively, as shown in Table 1. DCP is a weak acid and exists in solution in a non-dissociated form at pH below 7.80, whereas at pH above 7.8, it dissociates and converts to chlorophenolate. The same is true for 2,4-D; in solution at $\text{pH} < \text{pKa}$ (2.98), it

Table 6. Adsorption capacities of DCP and 2,4-D on activated carbons obtained from end-of-life tires compared to the literature data.

Adsorbent	S_{BET} [m^2/g]	Adsorption capacity, q_m [mmol/g]		Ref.
		DCP	2,4-D	
AC1:2	277	0.582	0.733	This paper
AC1:3	298	0.609	0.937	This paper
AC1:4	352	0.739	1.035	This paper
Carbopack B carbon black	97	0.288	0.309	Kuśmierek et al., 2016
Vulcan XC 72 carbon black	227	0.420	0.325	Kuśmierek et al., 2016
Carbonaceous material C-C ₂ Cl ₆	99	0.265	0.298	Kuśmierek et al., 2016
Carbonaceous material C-C ₆ Cl ₆	228	0.503	0.403	Kuśmierek et al., 2016
ROW 0.8Supra AC (Norit)	1089	1.343	1.588	Białek et al., 2017
Organosorb-10 AC (Desotec)	1049	1.307	1.517	Białek et al., 2017
D43/1 AC (Carbo-Tech)	1032	1.251	1.397	Białek et al., 2017
Tire pyrolysis char (ATPC-1)	70	0.135	–	Kuśmierek et al., 2020a
Tire pyrolysis char (ATPC-2)	155	0.167	–	Kuśmierek et al., 2020a
Tire pyrolysis char (ATPC-3)	255	0.295	–	Kuśmierek et al., 2020a
Template-synthesized carbon	399	0.667	–	Li and Zhang, 2019
Commercial AC Merck	760	2.067	–	Carmona et al., 2014
Commercial AC Prolabo	929	2.272	–	Hamdaoui and Naffrechoux, 2007
Oxidized carbon black N-220	82	–	0.124	Legocka et al., 2022
Carbon black N-220	108	–	0.138	Legocka et al., 2022
APTES-modified carbon black N-220	95	–	0.340	Legocka et al., 2022
Commercial AC F-400	800	–	0.620	Kim et al., 2008
Commercial AC SX2 Norit	870	–	1.211	Kuśmierek et al., 2020b
Commercial AC Sorbo Norit (S)	1225	–	1.490	Abdel Daiem et al., 2015
Commercial AC Ceca AC40 (C)	1201	–	1.560	Abdel Daiem et al., 2015
Commercial AC F-400	995	–	1.596	Kuśmierek et al., 2020b

exists in a non-dissociated (neutral) form, while in solution at $\text{pH} > \text{pKa}$, it dissociates. With increasing pH, more and more 2,4-D molecules dissociate, and at $\text{pH} \sim 5$, it is practically 100% in the anionic form (Abdel Daiem et al., 2015).

Knowledge of these two parameters (pH_{pzc} and pKa) can be helpful in understanding and explaining the effect of solution pH on the adsorption of DCP and 2,4-D on scrap tire-derived activated carbons, as shown in Fig. 7.

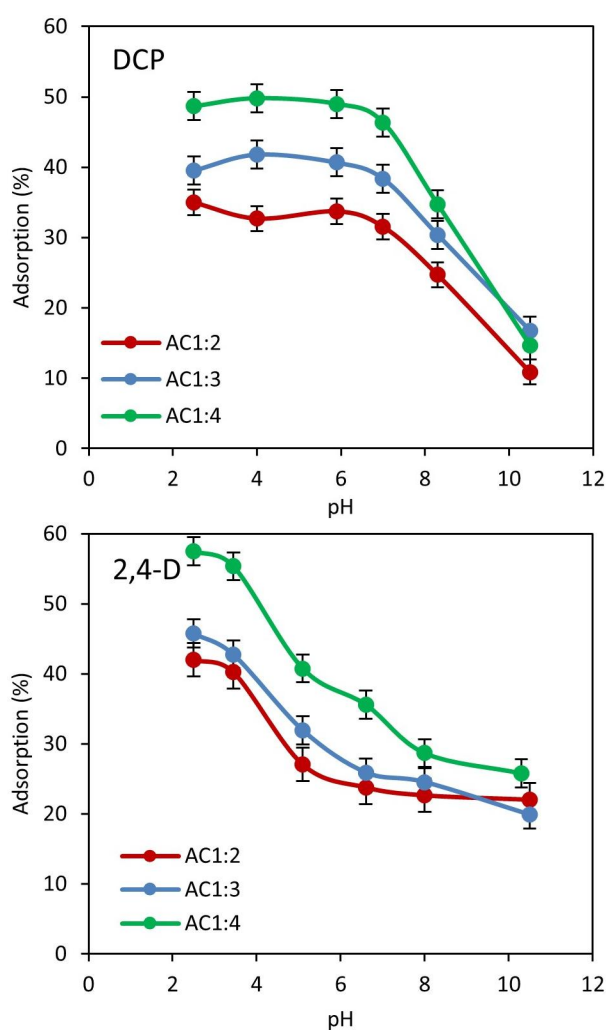


Figure 7. Effect of initial pH on the adsorption of DCP and 2,4-D on ACs produced from end-of-life tires. Experimental conditions: a DCP and 2,4-D initial concentrations = 0.5 mmol/L, AC dosage = 0.5 g/L, temperature = 23 °C.

The DCP adsorption on all three ACs (Fig. 7a) was more or less constant in the pH range from 2.5 to about 7. Further increases in pH resulted in a significant decrease in adsorption. When the pH of the solution was increased from 7 to 10, the adsorption efficiency decreased from 31.5% to 10.9% for AC1:2, from 38.4% to 16.7% for AC1:3, and from 46.5% to 14.7% for AC1:4. Thus, DCP was best adsorbed in an acidic environment, suggesting that the interaction of

a neutral (undissociated) chlorophenol molecule (below pKa) with a positively charged adsorbent surface (below pH_{pzc}) is most favored. An alkaline environment causes dissociation of the DCP molecule and accumulates a negative charge on the AC surface. Therefore, the decrease in adsorption efficiency observed in an alkaline environment is most likely due to repulsive electrostatic interactions between the negatively charged adsorbent surface and the adsorbate molecules in anionic form. These observations agree with those of other authors who reported a similar behavior of DCP adsorption as a function of the solution pH (Kuśmierek et al., 2016; Kuśmierek et al., 2020a; Li and Zhang, 2019).

The concept of adsorbent-adsorbate electrostatic interactions also explains the adsorption of 2,4-D from solutions with different initial pH, as shown in Figure 7b. As can be seen, 2,4-D was most effectively adsorbed at the initial (acidic) pH. Further increases in solution pH resulted in a gradual decrease in adsorption efficiency. When the pH was varied from 2.5 to 10.5, the adsorption efficiency decreased from 42% to 22% for AC1:2, from 45.8% to 19.9% for AC1:3, and from 55.7% to 26.5% for AC1:4. The herbicide was preferentially adsorbed at pH 2.5, i.e., when it was present in a neutral (non-dissociated) form and when the surface of the activated carbon was positively charged. The lowest adsorption efficiency of 2,4-D observed at pH 10.5, as in the case of DCP, resulted from repulsive electrostatic interactions between the adsorbate and the adsorbent, which were equally charged (negative). A similar trend in the adsorption of 2,4-D – a decrease in adsorption efficiency with increasing pH – has been reported elsewhere, e.g., on various activated carbons (Abdel Daiem et al., 2015), carbon blacks (Kuśmierek et al., 2016; Legocka et al., 2022), or carbon materials obtained by combustion synthesis (Kuśmierek et al., 2016).

4. CONCLUSIONS

In this paper, three activated carbons obtained from end-of-life tires were synthesized and characterized. The activated carbons were prepared with different ratios of tire pyrolysis char (TPC) to the activation agent (1:2, 1:3, and 1:4), which was KOH. Above mentioned ratios strongly influence the porous structure of obtained activated carbons. A very short activation time (15 min) was used to minimize the final material's production cost. The obtained ACs were used as adsorbents for the removal of chloroorganic contaminants from water. The 2,4-dichlorophenol (DCP) and the 2,4-dichlorophenoxyacetic acid (2,4-D) were chosen as model pollutants. Adsorption kinetics, adsorption isotherms, and the impact of solution pH were investigated. Results demonstrated that both adsorbates' adsorption kinetics followed the pseudo-second-order model and was controlled by film diffusion. The equilibrium adsorption data were modeled with Freundlich and Langmuir equations, and results showed that the Langmuir equation better described it. The Langmuir's maximum adsorption capacity

(q_m) of DCP adsorbed on AC1:2, AC1:3, and AC1:4 at equilibrium was 0.582, 0.609, and 0.739 mmol/g, respectively, while q_m values for 2,4-D were 0.733, 0.937, and 1.035 mmol/g, respectively. The adsorption equilibrium parameters q_m were good correlated with the porous structure parameters such as S_{BET} and V_{mi} of the tested activated carbons. Similar correlation was observed in the case of adsorption kinetics. The adsorption of both the adsorbates was pH-dependent. The results show that the scrap tire-derived ACs could be used as alternative low-cost adsorbents for the removal of chlorinated organic water contaminants such as DCP and 2,4-D.

SYMBOLS

B_T	mathematical function of q_t/q_e (the Boyd constant)
C_0	initial concentration of the adsorbate, mmol/L
C_{BET}	constant from the BET equation
C_e	equilibrium concentration of the adsorbate in solution, mmol/L
C_t	concentration of the adsorbate after time t , mmol/L
k_1	the pseudo-first-order adsorption rate constant, 1/min
k_2	the pseudo-second-order adsorption rate constant, g/mmol/min
K_F	Freundlich isotherm constant, (mmol/g)(L/mmol) ^{1/n}
K_L	Langmuir isotherm constant, L/mmol
m	mass of the activated carbon, g
n	Freundlich isotherm constants
q_e	adsorption capacity at equilibrium, mmol/g
$q_{e(\text{cal})}$	adsorption capacity model-predicted value, mmol/g
$q_{e(\text{exp})}$	experimental adsorption capacity, mmol/g
q_m	Langmuir maximum adsorption capacity, mmol/g
q_t	adsorption capacity at time t , mmol/g
R	universal gas constant, 8.314 J/mol·K
R^2	determination coefficient
R_L	separation factor
S_{BET}	specific surface area, m ² /g
T	temperature, K
t	time, min
V	volume of the solution, L
V_{me}	mesopore volume, cm ³ /g
V_{mi}	micropore volume, cm ³ /g
V_t	total pore volume, cm ³ /g
ΔG°	the Gibbs free energy of change, kJ/mol
χ^2	chi-square parameter

REFERENCES

- Abdel Daiem M.M., Rivera-Utrilla J., Sánchez-Polo M., Ocampo-Pérez R., 2015. Single, competitive, and dynamic adsorption on activated carbon of compounds used as plasticizers and herbicides. *Sci. Total Environ.*, 537, 335–342. DOI: [10.1016/j.scitotenv.2015.07.131](https://doi.org/10.1016/j.scitotenv.2015.07.131).
- Alexandre-Franco M., Fernández-González C., Alfaro-Domínguez M., Gómez-Serrano V., 2011. Adsorption of cadmium on carbonaceous adsorbents developed from used tire rubber. *J. Environ. Manage.*, 92, 2193–2200. DOI: [10.1016/j.jenvman.2011.04.001](https://doi.org/10.1016/j.jenvman.2011.04.001).
- Ali U.F.M., Hussin F., Gopinath S.C.B., Aroua M.K., Khamidun M.H., Jusoh N., Ibrahim N., Ahmad S.F.K., 2022. Advancement in recycling waste tire activated carbon to potential adsorbents. *Environ. Eng. Res.*, 27, 210452. DOI: [10.4491/eer.2021.452](https://doi.org/10.4491/eer.2021.452).
- Białek A., Kuśmierk K., Świątkowski A., 2017. Adsorption and desorption of phenol, 2,4-dichlorophenol and 2,4-dichlorophenoxyacetic acid from aqueous solutions on activated carbons. *Przem. Chem.*, 96, 2140–2144. DOI: [10.15199/62.2017.10.24](https://doi.org/10.15199/62.2017.10.24).
- Blachnio M., Kusmierk K., Swiatkowski A., Derylo-Marczewska A., 2023a. Adsorption of phenoxyacetic herbicides from water on carbonaceous and non-carbonaceous adsorbents. *Molecules*, 28, 5404. DOI: [10.3390/molecules28145404](https://doi.org/10.3390/molecules28145404).
- Blachnio M., Kusmierk K., Swiatkowski A., Derylo-Marczewska A., 2023b. Waste-based adsorbents for the removal of phenoxyacetic herbicides from water: a comprehensive review. *Sustainability*, 15, 16516. DOI: [10.3390/su152316516](https://doi.org/10.3390/su152316516).
- Boehm H.P., 2008. Chapter thirteen – Surface chemical characterization of carbons from adsorption studies. In: Bottani E.J., Tascón J.M.D. (Eds.), *Adsorption by carbons*. Elsevier, 301–327. DOI: [10.1016/B978-008044464-2.50017-1](https://doi.org/10.1016/B978-008044464-2.50017-1).
- Carmona M., Garcia M.T., Carnicer A., Madrid M., Rodríguez J.F., 2014. Adsorption of phenol and chlorophenols onto granular activated carbon and their desorption by supercritical CO₂. *J. Chem. Technol. Biotechnol.*, 89, 1660–1667. DOI: [10.1002/jctb.4233](https://doi.org/10.1002/jctb.4233).
- Crini G., Lichtfouse E., Wilson L.D., Morin-Crini N., 2019. Conventional and non-conventional adsorbents for wastewater treatment. *Environ. Chem. Lett.*, 17, 195–213. DOI: [10.1007/s10311-018-0786-8](https://doi.org/10.1007/s10311-018-0786-8).
- Czaplicka M., 2004. Sources and transformations of chlorophenols in the natural environment. *Sci. Total Environ.*, 322, 21–39. DOI: [10.1016/j.scitotenv.2003.09.015](https://doi.org/10.1016/j.scitotenv.2003.09.015).
- Dąbrowski A., Podkościelny P., Hubicki Z., Barczak M., 2005. Adsorption of phenolic compounds by activated carbon – a critical review. *Chemosphere*, 58, 1049–1070. DOI: [10.1016/j.chemosphere.2004.09.067](https://doi.org/10.1016/j.chemosphere.2004.09.067).
- Doczekalska B., Bartkowiak M., Łopatka H., Zborowska M., 2022. Activated carbon prepared from corn biomass by chemical activation with potassium hydroxide. *BioResour.*, 17, 1794–1804. DOI: [10.15376/biores.17.1.1794-1804](https://doi.org/10.15376/biores.17.1.1794-1804).
- Doczekalska B., Bartkowiak M., Waliszewska B., Orszulak G., Ceraży-Waliszewska J., Pniewski T., 2020. Characterization of chemically activated carbons prepared from miscanthus and switchgrass biomass. *Materials*, 13, 1654. DOI: [10.3390/ma13071654](https://doi.org/10.3390/ma13071654).
- Garba Z.N., Zhou W., Lawan I., Xiao W., Zhang M., Wang L., Chen L., Yuan Z., 2019. An overview of chlorophenols as contaminants and their removal from wastewater by adsorption: a review. *J. Environ. Manage.*, 241, 59–75. DOI: [10.1016/j.jenvman.2019.04.004](https://doi.org/10.1016/j.jenvman.2019.04.004).

- Hamdaoui O., Naffrechoux E., 2007. Modeling of adsorption isotherms of phenol and chlorophenols onto granular activated carbon: Part I. Two-parameter models and equations allowing determination of thermodynamic parameters. *J. Hazard. Mater.*, 147, 381–394. DOI: [10.1016/j.jhazmat.2007.01.021](https://doi.org/10.1016/j.jhazmat.2007.01.021).
- Hashimoto M., Taniguchi S., Takanami R., Giri R.R., Ozaki H., 2010. Oxidative degradation of 2,4-dichlorophenoxyacetic acid (2,4-D) in subcritical and supercritical waters. *Water Sci. Technol.*, 62, 484–490. DOI: [10.2166/wst.2010.329](https://doi.org/10.2166/wst.2010.329).
- Ighalo J.O., Ojukwu V.E., Umeh C.T., Aniagor C.O., Chinyelu C.E., Ajala O.J., Dulta K., Adeola A.O., Rangabhashiyam S., 2023. Recent advances in the adsorptive removal of 2,4-dichlorophenoxyacetic acid from water. *J. Water Proc. Eng.*, 56, 104514. DOI: [10.1016/j.jwpe.2023.104514](https://doi.org/10.1016/j.jwpe.2023.104514).
- Jedynak K., Charnas B., 2024. Adsorption properties of biochars obtained by KOH activation. *Adsorption*, 30, 167–183. DOI: [10.1007/s10450-023-00399-7](https://doi.org/10.1007/s10450-023-00399-7).
- Jones I., Zhu M., Zhang J., Zhang Z., Preciado-Hernandez J., Gao J., Zhang D., 2021. The application of spent tyre activated carbons as low-cost environmental pollution adsorbents: a technical review. *J. Cleaner Prod.*, 312, 127566. DOI: [10.1016/j.jclepro.2021.127566](https://doi.org/10.1016/j.jclepro.2021.127566).
- Kim T.-Y., Park S.-S., Kim S.-J., Cho S.-Y., 2008. Separation characteristics of some phenoxy herbicides from aqueous solution. *Adsorption*, 14, 611–619. DOI: [10.1007/s10450-008-9129-6](https://doi.org/10.1007/s10450-008-9129-6).
- Kuśmierk K., Pakuła M., Biniak S., Świątkowski A., Dąbek L., 2020b. Adsorption and electrodegradation of phenoxyacetic acids on various activated carbons. *Int. J. Electrochem. Sci.*, 15, 5770–5781. DOI: [10.20964/2020.06.25](https://doi.org/10.20964/2020.06.25).
- Kuśmierk K., Szala M., Świątkowski A., 2016. Adsorption of 2,4-dichlorophenol and 2,4-dichlorophenoxyacetic acid from aqueous solution on carbonaceous materials obtained by combustion synthesis. *J. Taiwan Inst. Chem. Eng.*, 63, 371–378. DOI: [10.1016/j.jtice.2016.03.036](https://doi.org/10.1016/j.jtice.2016.03.036).
- Kuśmierk K., Świątkowski A., Kotkowski T., Cherbański R., Molga E., 2021a. Adsorption on activated carbons from end-of-life tyre pyrolysis for environmental applications. Part I. preparation of adsorbent and adsorption from gas phase. *J. Anal. Appl. Pyrolysis*, 157, 105205. DOI: [10.1016/j.jaap.2021.105205](https://doi.org/10.1016/j.jaap.2021.105205).
- Kuśmierk K., Świątkowski A., Kotkowski T., Cherbański R., Molga E., 2020a. Adsorption properties of activated tire pyrolysis chars for phenol and chlorophenols. *Chem. Eng. Technol.*, 43, 770–780. DOI: [10.1002/ceat.201900574](https://doi.org/10.1002/ceat.201900574).
- Kuśmierk K., Świątkowski A., Kotkowski T., Cherbański R., Molga E., 2021b. Adsorption on activated carbons from end-of-life tyre pyrolysis for environmental applications. Part II. Adsorption from aqueous phase. *J. Anal. Appl. Pyrolysis*, 158, 105206. DOI: [10.1016/j.jaap.2021.105206](https://doi.org/10.1016/j.jaap.2021.105206).
- Legocka I., Kuśmierk K., Świątkowski A., Wierzbicka E., 2022. Adsorption of 2,4-D and MCPA herbicides on carbon black modified with hydrogen peroxide and aminopropyltriethoxysilane. *Materials*, 15, 8433. DOI: [10.3390/ma15238433](https://doi.org/10.3390/ma15238433).
- Li Y., Zhang N., 2019. Adsorption of phenol and 2,4-dichlorophenol from wastewater: kinetic and equilibrium studies. *Desalin. Water Treat.*, 170, 225–238. DOI: [10.5004/dwt.2019.24724](https://doi.org/10.5004/dwt.2019.24724).
- Moszczyński W., Białek A., 2012. Ecological production technology of phenoxyacetic herbicides MCPA and 2,4-D in the highest world standard. In: Hasaneen M.N., (Ed.), *Herbicides – properties, synthesis and control of weeds*. Intech. DOI: [10.5772/32140](https://doi.org/10.5772/32140).
- Mui E.L.K., Ko D.C.K., McKay G., 2004. Production of active carbons from waste tyres – a review. *Carbon*, 42, 2789–2805. DOI: [10.1016/j.carbon.2004.06.023](https://doi.org/10.1016/j.carbon.2004.06.023).
- Muttill N., Jagadeesan S., Chanda A., Duke M., Singh S.K., 2023. Production, types, and applications of activated carbon derived from waste tyres: an overview. *Appl. Sci.*, 13, 257. DOI: [10.3390/app13010257](https://doi.org/10.3390/app13010257).
- Nandi R., Jha M.K., Guchhait S.K., Sutradhar D., Yadav S., 2023. Impact of KOH activation on rice husk derived porous activated carbon for carbon capture at flue gas alike temperatures with high CO₂/N₂ selectivity. *ACS Omega*, 8, 4802–4812. DOI: [10.1021/acsomega.2c06955](https://doi.org/10.1021/acsomega.2c06955).
- Nasser S.M., Abbas M., Trari M., 2024. Understanding the rate-limiting step adsorption kinetics onto biomaterials for mechanism adsorption control. *Prog. React. Kinet. Mech.*, 49, 1–26. DOI: [10.1177/14686783241226858](https://doi.org/10.1177/14686783241226858).
- Ramírez-Arias A.M., Moreno-Piraján J.C., Giraldo L., 2020. Adsorption of Triton X-100 in aqueous solution on activated carbon obtained from waste tires for wastewater decontamination. *Adsorption*, 26, 303–316. DOI: [10.1007/s10450-019-00157-8](https://doi.org/10.1007/s10450-019-00157-8).
- Szymański G.S., Karpiński Z., Biniak S., Świątkowski A., 2002. The effect of the gradual thermal decomposition of surface oxygen species on the chemical and catalytic properties of oxidized activated carbon. *Carbon*, 40, 2627–2639. DOI: [10.1016/S0008-6223\(02\)00188-4](https://doi.org/10.1016/S0008-6223(02)00188-4).
- Tan K.L., Hameed B.H., 2017. Insight into the adsorption kinetics models for the removal of contaminants from aqueous solutions. *J. Taiwan Inst. Chem. Eng.*, 74, 25–48. DOI: [10.1016/j.jtice.2017.01.024](https://doi.org/10.1016/j.jtice.2017.01.024).
- Thommes M., Kaneko K., Neimark A.V., Olivier J.P., Rodriguez-Reinoso F., Rouquerol J., Sing K.S.W., 2015. Physisorption of gases, with special reference to the evaluation of surface area and pore size distribution (IUPAC Technical Report). *Pure Appl. Chem.*, 87, 1051–1069. DOI: [10.1515/pac-2014-1117](https://doi.org/10.1515/pac-2014-1117).
- WHO, 2003a. Chlorophenols in drinking water, Background document for development of WHO guidelines for drinking-water quality. WHO/SDE/WSH/03.04/47, World Health Organization, Geneva, 2003.
- WHO, 2003b. 2,4-D in drinking water, Background document for development of WHO guidelines for drinking-water quality. WHO/SDE/WSH/03.04/70, World Health Organization, Geneva, 2003.
- Yadav S., Kumar S., Haritash A.K., 2023. A comprehensive review of chlorophenols: fate, toxicology and its treatment. *J. Environ. Manage.*, 342, 118254. DOI: [10.1016/j.jenvman.2023.118254](https://doi.org/10.1016/j.jenvman.2023.118254).
- Zerin N.H., Rasul M.G., Jahirul M.I., Sayem A.S.M., 2023. End-of-life tyre conversion to energy: a review on pyrolysis and activated carbon production processes and their challenges. *Sci. Total Environ.*, 905, 166981. DOI: [10.1016/j.scitotenv.2023.166981](https://doi.org/10.1016/j.scitotenv.2023.166981).

Zerin N.H., Rasul M.G., Jahirul M.I., Sayem A.S.M., Haque R., 2024. Electrochemical application of activated carbon derived from end-of-life tyres: A technological review. *Sustainability*, 16, 47. DOI: [10.3390/su16010047](https://doi.org/10.3390/su16010047).

Zhang J., Gao J., Chen Y., Hao X., Jin X., 2017. Characterization, preparation, and reaction mechanism of hemp stem based activated carbon. *Results Phys.*, 7, 1628–1633. DOI: [10.1016/j.rinp.2017.04.028](https://doi.org/10.1016/j.rinp.2017.04.028).

Zhou X., Zhou X., 2014. The unit problem in the thermodynamic calculation of adsorption using the Langmuir equation. *Chem. Eng. Commun.*, 201, 1459–1467. DOI: [10.1080/00986445.2013.818541](https://doi.org/10.1080/00986445.2013.818541).